Microstructural Deformation Process of Shock-Compressed Polycrystalline Aluminum

The dynamic grain refinement of polycrystalline aluminum foil under laser-driven shockwave loading has been investigated using time-resolved X-ray diffraction. Diffraction spots on the Debye-Scherrer rings from micrometer-sized aluminum grains appeared and disappeared irregularly, because of grain rotation and subsequent size reduction. Besides, each diffraction spot was shifted and broadened as a result of laser-induced shockwave loading. The width distribution of the diffraction spots was broadened by the shock-induced grain refinement and microstrain in each shocked grain. We analyzed the in situ inhomogeneous lattice strain and grain size in the shocked polycrystalline aluminum using the Williamson-Hall method.

Microstructural deformation, grain refinement, and rotation in polycrystalline metal materials under shock compression are important characteristics for evaluating material strength and plastic deformation at a high strain rate. The shock-induced plastic deformation process in polycrystalline materials is different from those in single crystals and amorphous materials. Besides, while a material is undergoing plastic flow, the shockwave can rapidly generate slip or twining in each grain at a high strain rate (>10^6 s^{-1}), and the dislocation density increases with shock compression. Laser-induced shockwaves have been used for grain refinement and surface work hardening in the peening technique. To date, microstructural deformation under shockwave loading has mainly been investigated in post-shock recovery experiments using transmission electron microscopy. The recovery samples are influenced by the residual high temperature in releasing shock pressure and shockwave reflection at the interface. Recently, the deformation process with increasing the slip and twining of shocked-compressed solid materials has been observed by Laue diffraction with broadband X-rays [1-3] and an X-ray free-electron laser [4]. The application of stroboscopic time-resolved X-ray diffraction using intense and broadband X-ray pulses enables in situ characterization of plastic deformation in shock-compressed polycrystalline materials.

We performed single-shot and time-resolved broadbandwidth X-ray diffraction measurements using the AR-NW14A beamline. We quantitatively analyzed the shock-compressed microstructure deformation of polycrystalline aluminum using time-resolved X-ray diffraction. Because of the broad bandwidth energy ($\Delta E/E$ = 1.45% at 15.6 keV) of the X-ray pulse, we were able to observe the dynamic process of grain refinement and fragmentation in the shock-compressed polycrystalline sample from the X-ray diffraction patterns. We applied the pump-probe X-ray diffraction technique using Nd:YAG laser which produces a shockwave into the sample. Details of the experimental setup are described in ref. [3]. The sample target was composed of two layers: a 99.9% polycrystalline pure aluminum foil and an ablator film of polyethylene terephthalate. The thickness of the Al foil and ablator was 50 and 25 μm, as shown in Fig. 1. The pulse widths of the X-ray and laser were 100 ps and 8 ns with a Gaussian temporal profile. The interval between the X-ray pulse and laser pulse was set to be 0 ns when 50% of the InGaAs photodiode signal from them agreed.

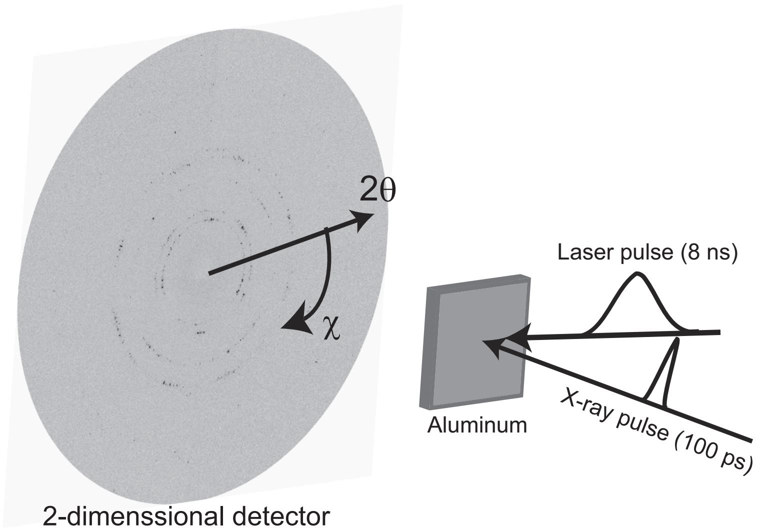

Figure 1: The experimental setup of single-shot time-resolved pink X-ray diffraction in the transmission X-ray diffraction geometry.

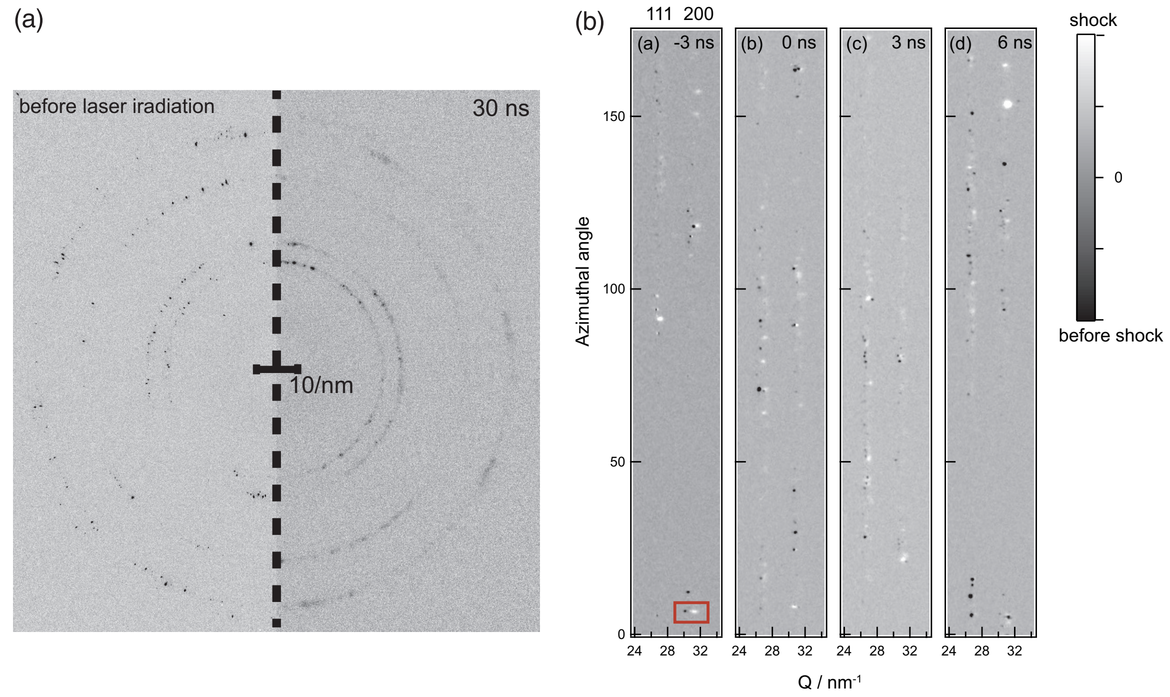

Figure 2: (a) Two-dimensional diffractogram of polycrystalline aluminum before laser irradiation (left image) and at 30 ns (right image). (b) Differential intensity from the Debye-Scherrer ring at −3, 0, 3, and 6 ns straightened into azimuthal-angle plots. The diffraction spot is broadened with shockwave propagation.

Figure 2(a) shows typical Debye-Scherrer rings from the polycrystalline aluminum foil at ambient pressure (left image) and at 30 ns after the laser irradiation (right image). The features in the diffraction rings in the azimuthal-angle direction become significantly smoother after shockwave propagation at 30 ns. The number of diffraction spots and broadening increased because of laser-shock fragmentation, which causes the formation of dislocation networks, subgrains, intergranular stress, and grain fracture. The peak pressure of the pressure profile, which was obtained from the free surface velocity using the velocimetry interferometer system of any reflector, was 8.4 GPa. The diffraction peak widths of each diffraction spot represented the grain refinement during and after shockwave-induced elastic-plastic deformation. The spottiness in the diffraction pattern changed as a function of delay time as shown in Fig. 2(b), where the differential aluminum 111 and 200 Debye Scherrer rings were straightened to the azimuthal angle; each diffraction spot corresponds to an individual grain. A few Bragg spots shifted to the high Q side at t = −3 ns, whereas others did not do so because those diffraction spots were affected by the shockwave loading. The shockwave front, generated from the tail of the laser temporal profile, entered the sample before 0 ns. The elastically deformed grains were located just behind the shockwave front. After t = 0 ns, the plastic shockwave mainly deformed the sample and reduced the size of each aluminum grain on a sub-nanosecond time scale with diffraction peak broadening. We estimated the coherent grain size and the inhomogeneous lattice strain under shockwave loading from the radial-width distribution of the diffraction spots using the Williamson-Hall approach. Upon compression at 6 ns, the diffraction peak broadening analysis based on the Williamson-Hall plot yields a grain size, inhomogeneous strain, and dislocation density of 33 nm, 0.21 × 10^{-2}, and 0.77 × 10^{15} m^{-2}, respectively [3]. We demonstrated the ability to study microstructural deformation in plastic shock flows from the atomic to the mesoscale level under shockwave loading.

REFERENCES

[1] K. Ichiyanagi, S. Adachi, S. Nozawa, Y. Hironaka, K.G. Nakamura, T. Sato. A. Tomita and S. Koshihara, *Appl. Phys. Lett.* **91**, 231918 (2007).
[2] K. Ichiyanagi and K.G. Nakamura, *Metals* **6**, 17 (2016).
[3] K. Ichiyanagi, S. Takagi, N. Kawai, R. Fukaya, S. Nozawa, K.G. Nakamura, K.-D. Liss, M. Kimura and S. Adachi, *Sci. Rep.* **9**, 7604 (2019).
[4] D. Milathianaki, S. Boutet, G.J. Williams, A. Higginbotham, D. Rathner, A.E. Gleason, M. Messerschmidt, M.M. Seibert, D.C. Swift, P. Hering, J. Robinson, W.E. White and J.S. Wark, *Science* **342**, 220 (2013).

BEAMLINE

AR-NW14A

K. Ichiyanagi[1], S. Takagi[1], N. Kawai[2], R. Fukaya[1], S. Nozawa[1], K. G. Nakamura[3], K.-D. Liss[4], M. Kimura[1] and S. Adachi[1] ([1]KEK-IMSS-PF, [2]Kumamoto Univ., [3]Tokyo Tech., [4]GTIT)